Biochimica et Biophysica Acta 1818 (2012) 1562–1569

Contents lists available at SciVerse ScienceDirect

Biochimica et Biophysica Acta

journal homepage: www.elsevier.com/locate/bbamem

Solution NMR spectroscopic characterization of human VDAC-2 in detergent micelles and lipid bilayer nanodiscs☆

Tsyr-Yan Yu [a], Thomas Raschle [a], Sebastian Hiller [b], Gerhard Wagner [a,*]

[a] Department of Biological Chemistry and Molecular Pharmacology, Harvard Medical School, 240 Longwood Ave., Boston, MA 02115, USA
[b] Biozentrum, University of Basel, Klingelbergstr. 70, 4056 Basel, Switzerland

ARTICLE INFO

Article history:
Received 1 September 2011
Received in revised form 27 October 2011
Accepted 7 November 2011
Available online 15 November 2011

Keywords:
VDAC
Mitochondrion
NMR spectroscopy
Micelle
Nanodisc
Membrane protein

ABSTRACT

Three isoforms of the human voltage-dependent anion channel (VDAC), located in the outer mitochondrial membrane, are crucial regulators of mitochondrial function. Numerous studies have been carried out to elucidate biochemical properties, as well as the three-dimensional structure of VDAC-1. However, functional and structural studies of VDAC-2 and VDAC-3 at atomic resolution are still scarce. VDAC-2 is highly similar to VDAC-1 in amino acid sequence, but has substantially different biochemical functions and expression profiles. Here, we report the reconstitution of functional VDAC-2 in lauryldimethylamine-oxide (LDAO) detergent micelles and 1,2-dimyristoyl-sn-glycero-3-phosphocholine (DMPC) lipid bilayer nanodiscs. We find that VDAC-2 is properly folded in both membrane-mimicking systems and that structural and functional characterization by solution NMR spectroscopy is feasible. This article is part of a Special Issue entitled: VDAC structure, function, and regulation of mitochondrial metabolism.

1. Introduction

The voltage-dependent anion channel (VDAC) is integral to the outer mitochondrial membrane (OMM), regulating the exchange of metabolites and ions between mitochondria and the cytosol. The number of VDAC isoforms is different among species, ranging from one in *Neurospora crassa*, two in *Saccharomyces cerevisiae*, three in *Homo sapiens*, four in *Drosophila melanogaster* up to five in *Lotus japonicus* [1,2]. Owing to its crucial function, VDAC has been studied extensively since its discovery in 1976 [3]. VDAC has also been implicated in the mitochondrial pathway of apoptosis, its role therein remains however controversial [4–8]. As a consequence, VDAC has also been viewed as a target for the development of novel drugs [9,10]. Early biochemical work in combination with bioinformatics analysis of the amino acid sequence, voltage-gating experiments and microscopic imaging techniques resulted in the proposal of several topology models of VDAC-1 [11]. These differences were resolved in 2008 by three independent determinations of the VDAC-1 3D structure. The use of three different approaches, i.e. solution NMR spectroscopy, X-ray crystallography and a hybrid approach employing both techniques, all led to the structure of VDAC-1 comprising 19 transmembrane β-strands [12–14]. The presence of 19 β-strands represents a unique structural class of β-barrel membrane proteins [11].

The amino acid sequence of human VDAC-2 is 68% identical to human VDAC-1. Despite this high sequence similarity, VDAC-2 has been reported to have distinct physiological roles and expression profiles [15]. In particular, VDAC-2 has been indicated to play an important role in the mitochondrial pathway of apoptosis as it was shown to regulate the activity of the pro-apoptotic BAK protein [16]. In addition, VDAC-2 has been identified as a target of the anti-tumor compound erastin. Erastin was shown to induce non-apoptotic cell death in some tumor cells harboring activating mutations in the RAS–RAF–MEK pathway [17,18]. In order to better understand the role of VDAC-2 in BAK mediated mitochondrial apoptosis, detailed structural information at atomic resolution is highly desired. In addition, insight into binding of erastin to VDAC-2 by mapping the interface might provide information for the generation of more efficient drugs.

Solution NMR spectroscopy has been successfully applied to characterize structural and functional properties of many membrane proteins including VDAC-1 [11,19–26]. Here, we show that VDAC-2, refolded into lauryldimethylamine-oxide (LDAO) detergent micelles or 1,2-dimyristoyl-sn-glycero-3-phosphocholine (DMPC) nanodiscs, is properly folded. Using solution NMR spectroscopy, we were able to identify specific sites for nicotinamide adenine dinucleotide (NADH) binding. Furthermore, our results indicate that the quality of refolded VDAC-2 in detergent micelles as well as in nanodiscs is suitable for its functional and structural characterization using solution NMR spectroscopy. VDAC-2 in nanodiscs might provide a unique opportunity to study the BAK–VDAC-2 complex under non-denaturing condition.

☆ This article is part of a Special Issue entitled: VDAC structure, function, and regulation of mitochondrial metabolism.

* Corresponding author. Tel.: +1 617 432 3213; fax: +1 617 432 4383.
E-mail address: gerhard_wagner@hms.harvard.edu (G. Wagner).

0005-2736/$ – see front matter © 2011 Elsevier B.V. All rights reserved.
doi:10.1016/j.bbamem.2011.11.012

2. Materials and methods

2.1. Expression of VDAC-2

The cDNA for human voltage-dependent anion channel isoform 2 (VDAC-2) with the GenBank accession number BC000165 was obtained as a full-length clone from the Mammalian Gene Collection (OpenBioSystems, Huntsville, AL). VDAC-2 with a C-terminal His-tag (VDAC-2(1–294)-Leu-Glu-His-His-His-His-His-His) was cloned by standard PCR methods into the NheI/XhoI sites of pET21d (Novagen). Site-directed mutagenesis was carried out to change the codons for the second and the third residues (Ala-Thr) of VDAC-2 to be GCTACT to have optimized protein expression Agilent Technologies. VDAC-2 was expressed in Rosetta 2(DE3) cells by induction with 1 mM IPTG (Gold Biotechnology) at 37 °C for 12 h.

2.2. Purification of VDAC-2

Cells were resuspended in lysis buffer (50 mM Tris–HCl, 250 mM NaCl, 5 mM 2-mercaptoethanol (Sigma), protease inhibitor cocktail tablets (Roche), pH 6.8) and lysed by sonication. The VDAC-2 containing inclusion bodies were isolated using sucrose cushion centrifugation (50 mM Tris–HCl, 500 mM NaCl, 50% sucrose, pH 6.8). The inclusion bodies were dissolved in denaturing buffer (8 M urea, 50 mM Tris–HCl, 100 mM NaCl, 20 mM imidazole, pH 7.5), applied to Ni-agarose resin (Qiagen) and VDAC-2 was eluted with elution buffer (8 M urea, 50 mM Tris–HCl, 100 mM NaCl, 250 mM imidazole, pH 7.0). Purified VDAC-2 in elution buffer was precipitated by dialysis against 4 l of dialysis buffer (50 mM Tris–HCl, 50 mM NaCl, 1 mM EDTA, 5 mM DTT, pH 7.0) in a 6000–8000 molecular weight cutoff (MWCO) dialysis membrane. Precipitated VDAC-2 was isolated by centrifugation at 12,000 *g*. The purity of the Ni-affinity purified VDAC-2 was checked with SDS page chromatography (Fig. 1).

2.3. Refolding and purification of VDAC-2 in LDAO detergent

Purified precipitated VDAC-2 was dissolved in guanidine hydrochloride buffer (100 mM NaP_i, 100 mM NaCl, 6 M GuHCl, 5 mM TCEP, 1 mM EDTA, pH 6.7) at a concentration of 3 mg/ml. VDAC-2 was refolded at 4 °C by dropwise dilution of one volume VDAC-2 solution into 10 volumes of refolding buffer (25 mM NaP_i, pH 6.8, 100 mM NaCl, 1 mM EDTA, 5 mM TCEP, 1.5% (64.5 mM) LDAO (Anatrace and FBReagents)) with stirring. The final ratio of VDAC-2 protein to LDAO micelles is about 1:90 assuming the aggregation number of LDAO micelle is 76. After overnight stirring at 4 °C the refolded VDAC-2 sample was dialyzed against 4 l of buffer (25 mM NaP_i, 1 mM EDTA, 5 mM DTT, pH 6.8) for 12 to 16 h. Little amount of precipitated VDAC-2 was removed using centrifugation at 12,000 *g*, followed by filtration with a 0.22-μm membrane.

Cation exchange chromatography was employed to isolate properly folded VDAC-2 protein in LDAO detergent micelles. The sample was loaded onto a 30 ml SP sepharose HP column equilibrated with buffer A (25 mM NaP_i, 1 mM EDTA, 5 mM DTT, 0.1% LDAO, pH 7.0). VDAC-2 was eluted during a 5%–55% gradient with buffer B (25 mM NaP_i, 1 mM EDTA, 5 mM DTT, 0.1% LDAO, 1 M NaCl, pH 6.2) at about 35% buffer B. Pure VDAC-2 fractions were pooled and concentrated to the desired concentration using 30 k molecular weight cutoff (MWCO) concentrators.

VDAC-2 was further purified by gel filtration chromatography using a superdex 200 prep grade column (GE Healthcare). The column was equilibrated in NMR buffer (25 mM NaP_i, 100 mM NaCl, 20 mM TCEP, 0.1% LDAO, EDTA 1 mM, pH 6.8). After final purification, the sample was concentrated using 10 k MWCO concentrator. The LDAO detergent concentration was monitored by 1D ^{1}H-NMR spectroscopy and adjusted by a series of dilution and concentration steps with buffer A. The final sample conditions were 25 mM NaP_i (pH 6.8), 100 mM NaCl, 20 mM TCEP, ~250 mM LDAO and 0.5–0.8 mM VDAC-2.

2.4. Incorporation of VDAC-2 in DMPC nanodiscs

Following the protocol for preparing VDAC-1 in DMPC nanodiscs [27], VDAC-2 was first refolded in LDAO detergent micelles and subsequently assembled into DMPC nanodiscs. The plasmid coding for the N-terminal deletion mutant (MSP1D1) of the membrane scaffold protein (MSP1) was obtained from the non-profit plasmid repository Addgene deposited by Stephen Sligar [28]. Expression and purification of MSP1D1 was essentially done as described in Ref. [28]. For the incorporation of VDAC-2 into nanodiscs, MSP1D1 protein, refolded VDAC-2 in LDAO detergent micelles and sodium cholate solubilized DMPC lipids were incubated for 1 h at room temperature prior to the removal of the detergents by the addition of biobeads SM2 (BioRad). The ratio of lipid to MSP1D1 was optimized by analytical size exclusion chromatography to account for displacement of lipid molecules by VDAC-2. A 1:8:640 ratio for VDAC-2/MSP1D1/DMPC lipid was found to yield the highest fraction of assembled nanodiscs. Reconstituted VDAC-2 embedded in nanodiscs was isolated by Ni-NTA affinity chromatography followed by size-exclusion chromatography onto a Superdex 200 prep grade gel filtration column (GE Healthcare) equilibrated in 25 mM NaP_i (pH 6.8), 100 mM NaCl, 0.5 mM EDTA. The final concentration of [*U*-^{2}H,^{15}N] VDAC-2 and [*U*-^{2}H,^{13}C,^{15}N] VDAC-2 was estimated to be ~200 and 500 μM, respectively.

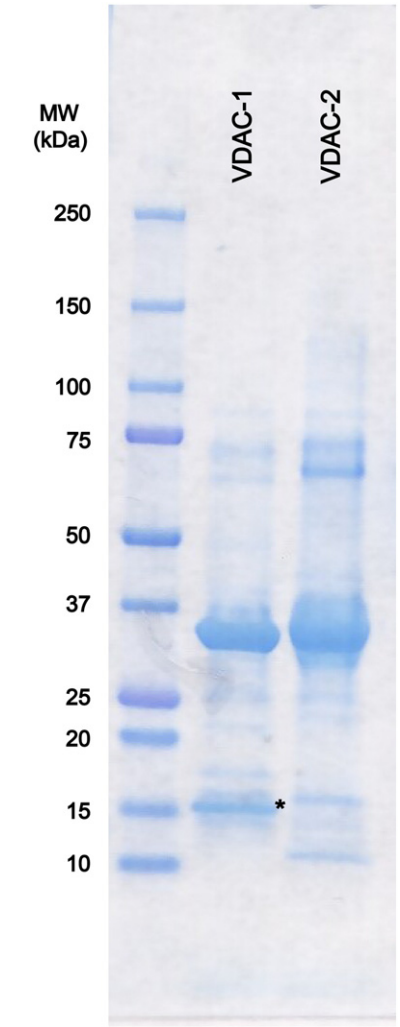

Fig. 1. SDS-PAGE gel of Ni-affinity purified VDAC-1 and VDAC-2. The 15-kDa truncation product of VDAC-1 [29] is indicated by a star sign.

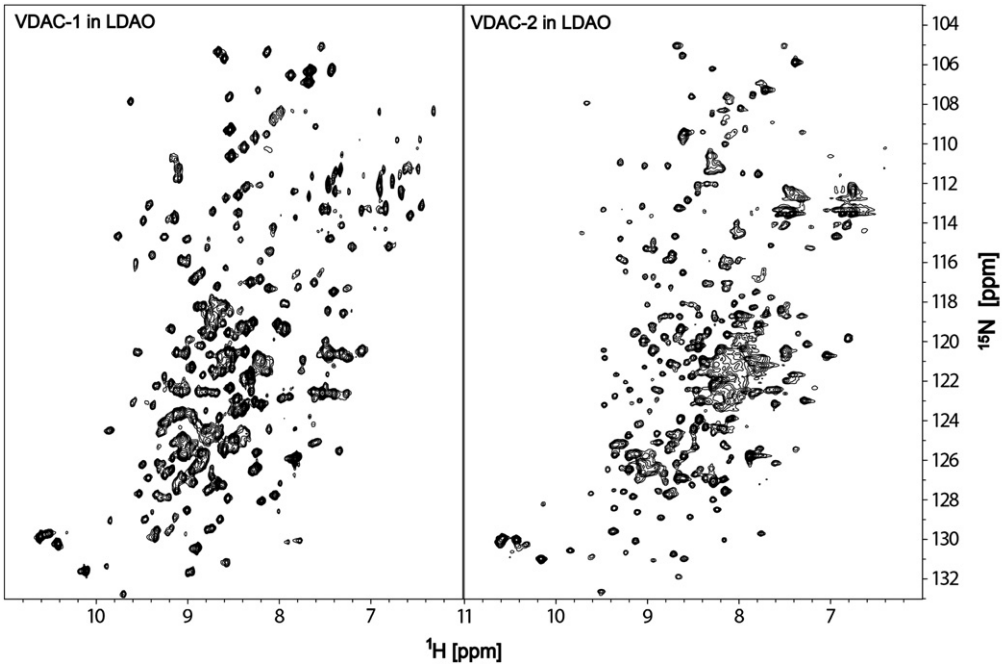

Fig. 2. Comparison of NMR spectra of VDAC-2 and VDAC-1 in LDAO detergent micelles. 2D [^{15}N,^{1}H]-TROSY spectrum of [*U*-^{2}H,^{15}N] VDAC-1 (left) and [*U*-^{2}H,^{13}C,^{15}N] VDAC-2 (right) in LDAO detergent micelles recorded on a Bruker 750 MHz spectrometer at 30 °C. 512 and 200 complex points were recorded in the direct and indirect dimensions, respectively. 8 transients were recorded, resulting in a total experiment time of 1 h for each spectrum. Protein concentrations for VDAC-2 and VDAC-1 were 800 μM (left) and 750 μM (right), respectively.

2.5. NMR spectroscopy

All NMR experiments were performed on Bruker spectrometers operating at field strengths of 750, 800 and 900 MHz. All spectrometers were equipped with cryogenically cooled probes. For VDAC-2 solubilized in LDAO detergent micelles, 2D [^{15}N,^{1}H]-TROSY, 3D TROSY-HNCA, 3D [^{1}H,^{1}H]-NOESY-^{15}N-TROSY and [^{15}N,^{1}H]-TRACT experiments [29] were recorded at 30 °C. For VDAC-2 embedded in DMPC nanodiscs, 2D [^{15}N,^{1}H]-TROSY, 3D [^{1}H,^{1}H]-NOESY-^{15}N-TROSY and [^{15}N,^{1}H]-TRACT experiments were acquired at 30 °C and 40 °C.

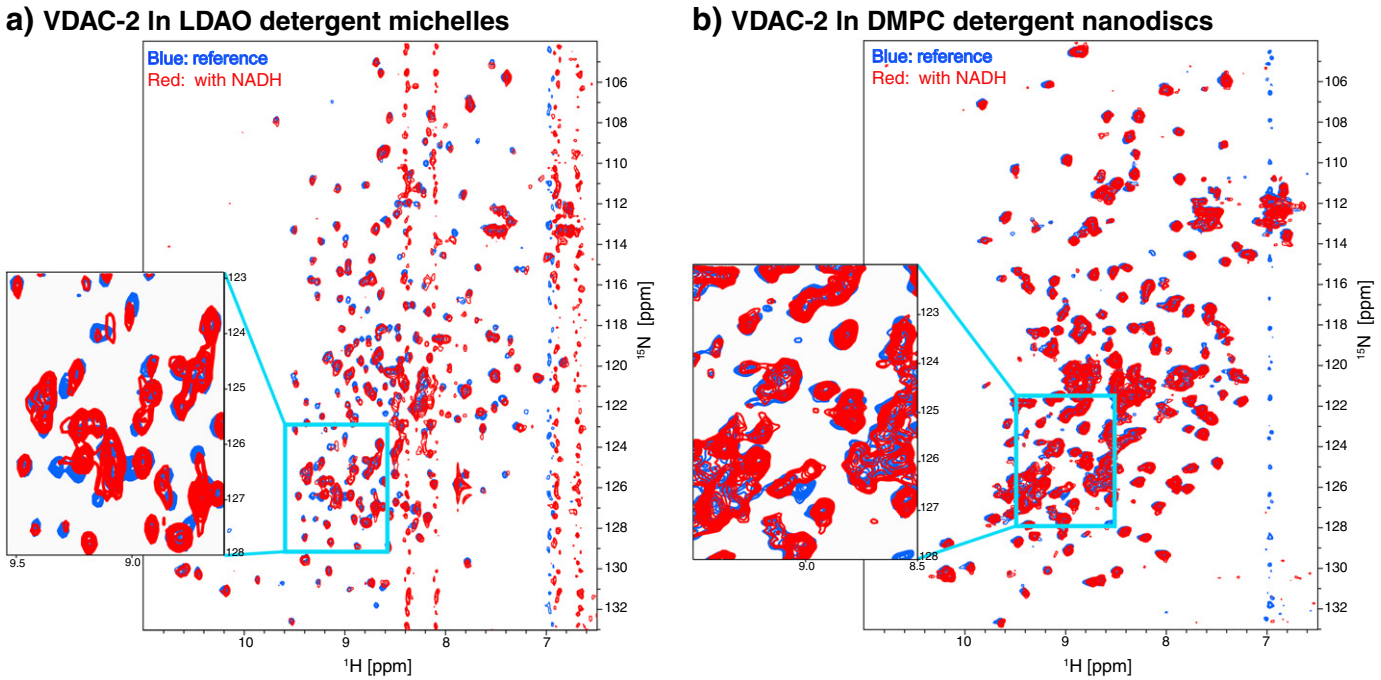

Fig. 3. NADH binding of VDAC-2. (a) NADH binding of VDAC-2 in LDAO detergent micelles. 2D [^{15}N,^{1}H]-TROSY spectra of a 250 μM sample of [*U*-^{2}H,^{15}N] VDAC-2 in 240 mM LDAO in the absence (blue) and in the presence of 100 mM NADH (red) at 30 °C. Spectra were recorded on a Bruker 900 MHz spectrometer. 512 and 128 complex points were recorded in the direct and indirect dimensions, respectively. 16 transients were recorded, resulting in a total experiment time of 1.1 h for each spectrum. (b) NADH binding of VDAC-2 embedded in DMPC nanodiscs. 2D [^{15}N,^{1}H]-TROSY spectra of a 200 μM sample of [*U*-^{2}H,^{15}N] VDAC-2 in DMPC nanodiscs in the absence (blue) and in the presence of 50 mM NADH (red) at 40 °C. Spectra were recorded on a Bruker 900 MHz spectrometer. 512 and 144 complex points were recorded in the direct and indirect dimensions, respectively. 240 transients were recorded, resulting in a total experiment time of 19.2 h for each spectrum.

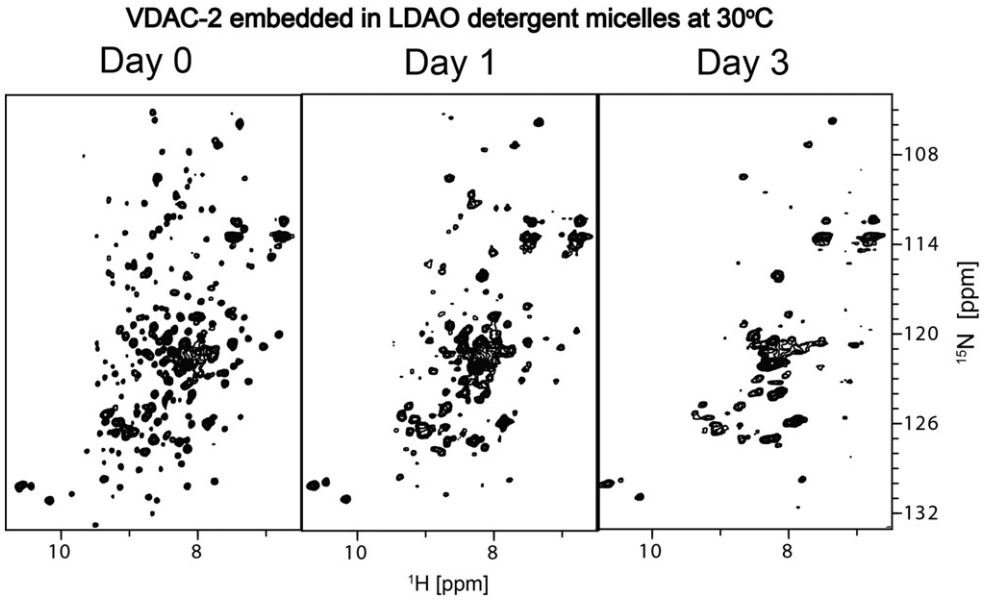

Fig. 4. Stability of VDAC-2 reconstituted in LDAO detergent micelles at 30 °C. 2D [^{15}N,^{1}H]-TROSY spectra of [*U*-^{2}H,^{15}N] VDAC-2 in LDAO detergent micelles recorded immediately after sample preparation, after 24 h and after 72 h, as indicated. Spectra were recorded on a Bruker 750 spectrometer. 512 and 128 complex points were recorded in the direct and indirect dimensions, respectively. 16 transients were recorded, resulting in a total experiment time of 1.1 h for each spectrum.

3. Results

3.1. Expression, purification, and refolding of VDAC-2

Several attempts were made to express VDAC-2 protein in BL21 cells. No detectable level of VDAC-2 protein was expressed in BL21(DE3) cells 6 h after induction. In contrast, expression of VDAC-2 protein in Rosetta 2(DE3) cells yielded 30 to 40 mg of protein per liter of M9 minimal medium in the insoluble *Escherichia coli* inclusion body fraction.

Purification of VDAC-2 using Ni-affinity chromatography yielded VDAC-2 protein with a purity above 90% (Fig. 1) that could be directly used for refolding. Whereas VDAC-1 typically contains a distinct 15 kDa truncation product as an impurity of up to 15% [30], such a truncation product was not observed for VDAC-2. Refolding of guanidine hydrochloride solubilized VDAC-2 was accomplished by dropwise dilution into buffer containing LDAO detergent with a refolding yield of 15–30%. Aggregated and misfolded VDAC-2 protein was removed by cation exchange chromatography and gel filtration chromatography.

3.2. Characterization of VDAC-2 in LDAO detergent micelles

In order to characterize VDAC-2 by solution NMR spectroscopy, the protein was perdeuterated and uniformly labeled with ^{15}N. [*U*-^{2}H,^{15}N] VDAC-2 in LDAO detergent micelles yielded a well-resolved 2D [^{15}N,^{1}H]-TROSY spectrum (Fig. 2 right), indicating the formation of extensive secondary structure. The comparison with the 2D [^{15}N,^{1}H]-TROSY spectrum of VDAC-1 (Fig. 2 left) shows that several similar patterns of well-dispersed resonances are observed in both spectra. NADH was reported to regulate the gating of VDAC [31,32], suggesting specific binding of NADH to well-folded VDAC proteins. To test for binding of NADH, 2D [^{15}N,^{1}H]-TROSY spectra were acquired before and after addition of NADH (Fig. 3a). Several distinct chemical shift changes were observed, indicating site-specific binding of NADH to VDAC-2. Our current sequence-specific resonance assignment data for VDAC-2 suggest that NADH binds to the same interaction interface as observed for VDAC-1 [12].

While VDAC-2 in LDAO yielded good quality spectra, a thorough characterization of VDAC-2 by solution NMR spectroscopy is impeded by the poor sample stability. In some cases, detergent-solubilized VDAC-2 was stable for about 1 week, which is sufficiently long to allow the acquisition of a 3D triple resonance experiment, such as the 3D TROSY-HNCA. In other preparations, however, VDAC-2 was stably folded for less than 3 days and it was not possible to record longer NMR experiments. A representative example is shown in Fig. 4. These spectra document the disappearance of many peaks below the noise level within 3 days. Further optimization of the NMR sample composition for better stability is thus required for characterizing VDAC-2 in LDAO with high-resolution NMR.

3.3. Characterization of VDAC-2 embedded in DMPC nanodiscs

To alleviate the stability problem we decided to explore the use of nanodiscs for structural and functional studies of VDAC-2. The protein was successfully transferred in DMPC nanodiscs using established protocols [27] and the resulting 2D [^{15}N,^{1}H]-TROSY spectra featured well-dispersed resonances. We then used the small ligand NADH to examine the activity of VDAC-2 embedded in DMPC nanodiscs. The 2D [^{15}N,^{1}H]-TROSY spectra of [*U*-^{2}H,^{15}N] VDAC-2 were recorded before and after addition of NADH. Several distinct chemical shift changes were clearly observed (Fig. 3b), suggesting that VDAC-2 embedded in DMPC nanodiscs is functional.

In order to determine a suitable temperature for NMR characterization, the effect of increasing temperature on the spectral quality and stability of VDAC-2 in nanodiscs was monitored. 2D [^{15}N,^{1}H]-TROSY spectra of [*U*-^{2}H,^{15}N] VDAC-2 embedded in DMPC nanodiscs were recorded at 30, 37, 40 and 45 °C (Fig. 5). The NMR sample was examined by eye after each 2D experiment recorded at the specified temperature. In addition, the intensities of the 1D ^{15}N-TROSY-filtered-^{1}H NMR spectra recorded before and after each 2D experiment were utilized to quantify the percentage of folded protein. No precipitation was found when 2D experiments were recorded at 30, 37 and 40 °C. The intensities of the 1D spectra also remained unchanged for a period of at least 20 h. However, at 45 °C small amounts of macroscopic precipitation were observed after a period of 20 h. In the same time period, the intensity of the 1D ^{15}N-TROSY-filtered-^{1}H NMR spectrum was found to be reduced by 10%. There are more than 240 peaks resolved in the 2D [^{15}N,^{1}H]-TROSY spectra acquired at 40 and 45 °C, but only less than 210 resonance peaks were resolved in those recorded at 30 and 37 °C. Considering the sample stability and the number of peaks resolved in 2D [^{15}N,^{1}H]-TROSY spectra, all

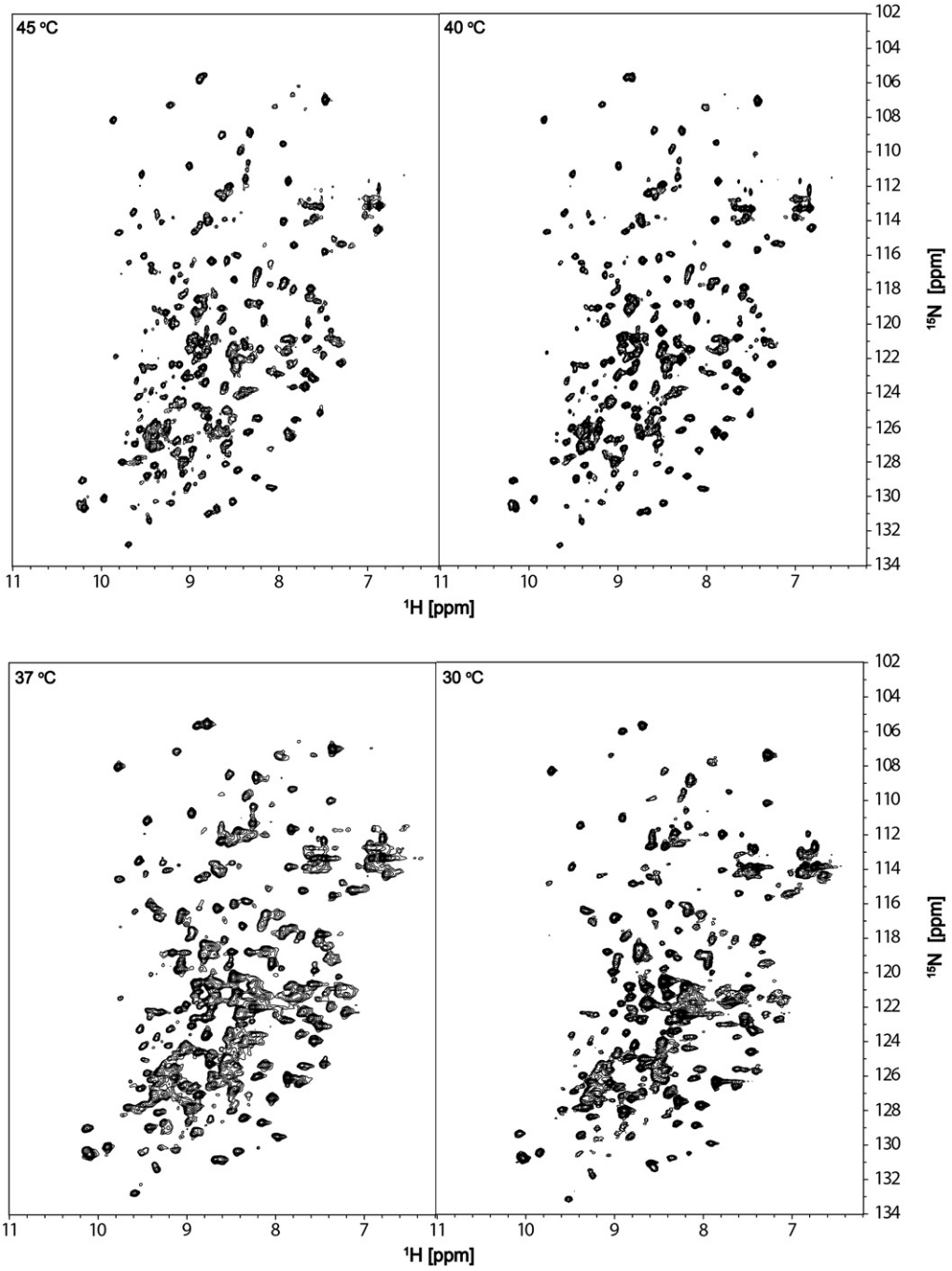

Fig. 5. Temperature stability of VDAC-2 embedded in DMPC nanodiscs. 2D [^{15}N,^{1}H]-TROSY spectra of [*U*-^{2}H,^{15}N] VDAC-2 in DMPC nanodiscs recorded at 30 °C, 37 °C, 40 °C and 45 °C as indicated. Spectra were recorded on a Bruker 800 spectrometer. 1024 and 160 complex points were recorded in the direct and indirect dimensions, respectively. 192 transients were recorded, resulting in a total experiment time of 19 h for each spectrum.

further NMR experiments were recorded at 40 °C. The rotational correlation time τ_c of VDAC-2 embedded in DMPC nanodiscs at 40 °C was determined to be 90 ± 15 ns (Fig. 6), corresponding to an effective overall molecular weight of 160–200 kDa. For comparison, τ_c was measured to be 95 ns when the TRACT experiment was performed at 30 °C, which is comparable to the reported τ_c of VDAC-1 embedded in DMPC nanodiscs [27].

3.4. Sequence-specific resonance assignments

In order to map the binding site of NADH on VDAC-2, the assignment of the protein backbone resonances is required. To evaluate the feasibility of the backbone assignment, 3D TROSY-HNCA and 3D [^{1}H,^{1}H]-NOESY-^{15}N-TROSY experiments of [*U*-^{2}H,^{13}C,^{15}N] VDAC-2 were recorded. Our results showed that the spectral quality of these 3D spectra is sufficiently high to allow the assignment of protein backbone resonances. Since 68% of the VDAC-2 amino acid sequence is identical to VDAC-1, the resonance assignment process is facilitated by comparing the 3D TROSY-HNCA spectra of VDAC-2 and VDAC-1. Currently, the sequence-specific resonance assignment for 50% of the backbone amide resonances of VDAC-2 in LDAO micelles has been established. An example of HNCA assignment strips is provided in Fig. 7 comparing equivalent segments from VDAC-1 and VDAC-2.

To evaluate the feasibility to assign the amide backbone resonances and to obtain structural information of VDAC-2 embedded in DMPC nanodiscs, a 3D HNCA triple resonance spectrum and a 3D

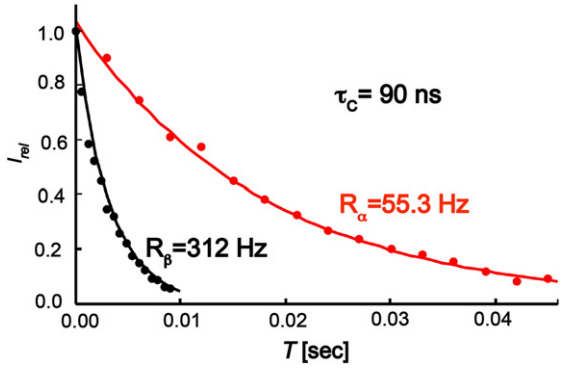

Fig. 6. [^{15}N,^{1}H]-TRACT experiment for the determination of the rotational correlation time τ_c. The 1D proton signal intensity, I_{rel}, was integrated over the region 8.0–10.5 ppm and plotted versus the relaxation period *T*. The transverse relaxation rates of the TROSY component (red) and the anti-TROSY component (black) were determined to be $R_\alpha = 55.3$ Hz and $R_\beta = 312$ Hz, respectively, corresponding to a rotational correlation time τ_c of 90 ns [28]. The experiment was recorded on a Bruker 900 MHz spectrometer in a total experiment time of 12 h.

[^{1}H,^{1}H]-NOESY-^{15}N-TROSY experiment were recorded at 40 °C. The 2D [^{1}H,^{1}H]-projection of the latter spectrum (Fig. 8) shows a large number of H^N–H^N NOESY cross peaks to be observable in this bilayer-like environment. These data also suggest that backbone resonance assignments and structure determination of VDAC-2 in lipid bilayer nanodiscs should be feasible.

4. Discussion

Biophysical studies of membrane proteins require finding suitable membrane-mimicking environments to maintain the proteins in a stable and active state. We have demonstrated that the 32-kDa human integral membrane protein VDAC-2 can be reconstituted into LDAO detergent micelles, as well as in DMPC nanodiscs in a functional form, as assessed by ligand binding. The latter membrane mimic resembles a phospholipid bilayer and is probably the closest mimic of a real membrane suitable for solution structure methods. We have also shown that 3D triple-resonance experiments for sequence-specific resonance assignments of VDAC-2 in both membrane mimetic systems are feasible. Most membrane proteins studied by solution NMR were reconstituted into detergent micelles. Very few proteins have been studied in both detergent micelles and phospholipid bilayers [33]. The present work offers an exciting opportunity to compare the structures and dynamics of VDAC-2 reconstituted in both membrane-mimicking environments.

VDAC-2 in LDAO detergent prepared using the current protocol was not as stable as VDAC-1 in the same detergent. This observation indicates that the protocol for preparing an NMR sample of VDAC-2 in LDAO detergent can be further optimized for better stability. Nonetheless, the currently established method already allowed us to

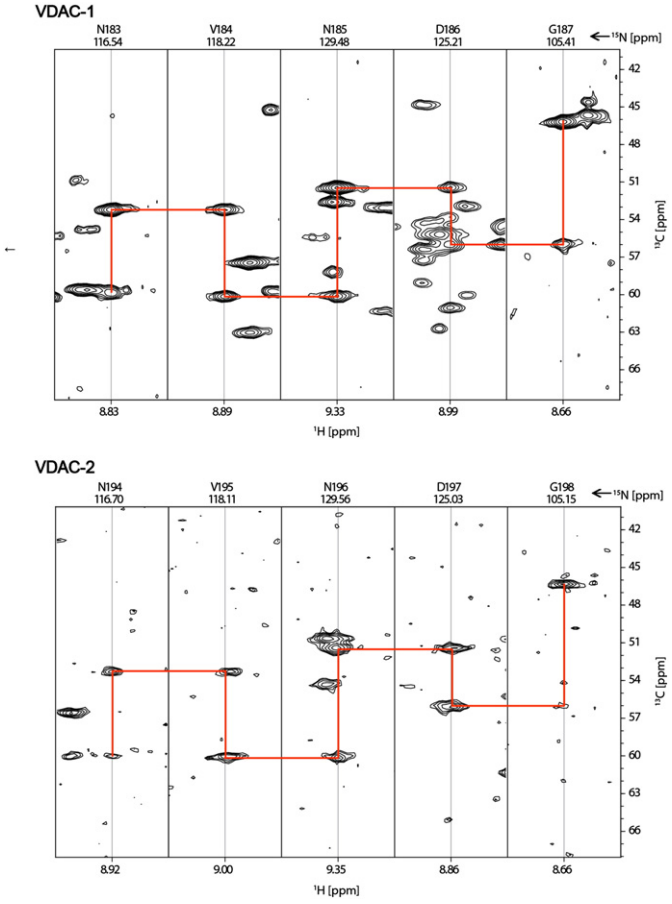

Fig. 7. Representative strips from two 3D TROSY-HNCA experiments. Strips for residues 183–187, corresponding to β-strand 12, from a 3D TROSY-HNCA experiment with [*U*-^{2}H,^{13}C,^{15}N] VDAC-1 in [*U*-^{2}H] LDAO (top). Strips for residues 194–198, corresponding to β-strand 12, from a 3D TROSY-HNCA experiment with [*U*-^{2}H,^{13}C,^{15}N] VDAC-2 in [*U*-^{2}H] LDAO (bottom). The red lines indicate the sequential connectivities between strips. Residues 183–187 of VDAC-1 correspond to residues 194–198 of VDAC-2 in a sequence alignment. This particular polypeptide segment features 100% sequence identity, as compared to 68% for the full proteins. The 3D TROSY-HNCA strips show a near identical pattern. Spectra were recorded on a Bruker 750 spectrometer. 1024/38/40 complex points were recorded in the three dimensions. 64 transients were recorded, resulting in a total experiment time of 108 h for each experiment.

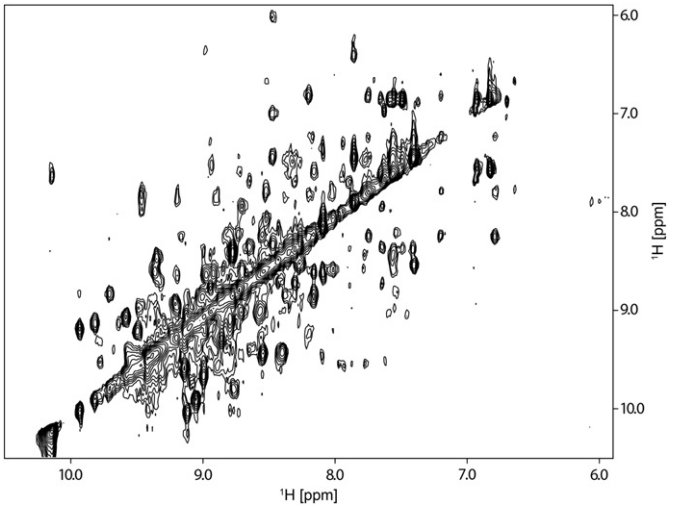

Fig. 8. 2D [^{1}H,^{1}H]-projection of a 3D [^{1}H,^{1}H]-NOESY-^{15}N-TROSY spectrum of [*U*-^{2}H,^{13}C,^{15}N] VDAC-2 embedded in DMPC nanodiscs. Numerous cross peaks can be detected besides the diagonal. The spectrum was recorded on a Bruker 900 MHz spectrometer. 1024/40/60 complex points were recorded in the three dimensions, respectively. 48 transients were recorded, resulting in a total experiment time of 154 h.

perform ligand-binding experiments and to record certain 3D triple resonance experiments for sequence-specific resonance assignment.

The resonance peaks of the 2D [^{15}N,^{1}H]-TROSY spectrum of VDAC-2 in nanodiscs display slightly broader line widths in the proton dimension when compared to VDAC-2 in LDAO. A similar result was also observed when comparing spectra of VDAC-1 in nanodiscs and spectra of VDAC-1 in LDAO detergent [28]. This is readily rationalized since the overall size of the VDAC–DMPC-nanodisc complex is larger than the size of the VDAC–LDAO-micelle complex, leading to slower molecular tumbling. Larger size of a protein complex is generally not favored for solution NMR studies. However, since the thermal stability of VDAC-2 in nanodiscs is better than in LDAO detergent, NMR experiments can be carried out at higher temperature. The higher measuring temperatures can at least partially compensate for the increased size. The high stability of VDAC-2 in lipid bilayer nanodiscs allowed us to perform NMR experiments at 40 °C. The quality of the 2D TROSY spectrum of VDAC-2 in nanodiscs at 40 °C is comparable to that of VDAC-2 in LDAO micelles at 30 °C (Figs. 2 and 7).

5. Conclusions

VDAC-2 was reconstituted in LDAO detergent micelles and in DMPC nanodiscs in a well-folded form. Our NMR results show that sequence-specific assignments are feasible for VDAC-2 in both membrane-mimicking systems. Further studies are required for mapping out the exact binding locations of NADH on VDAC-2. Functional VDAC-2 in DMPC nanodiscs provides a unique opportunity to study the complex of VDAC-2 and BAK, which in turn may provide information on the inhibition of BAK-mediated apoptotisis by VDAC-2.

Acknowledgements

T.-Y. Yu was supported in part by National Science Council in Taiwan (NSC98-2917-I-564-157). This research was supported by NIH (grants GM075879 and GM047467) and the Swiss National Science Foundation. S. Hiller was supported by ERC grant MOMP 281764. Purchase and maintenance of the instruments used for these studies were supported by NIH grants S10 RR026417 and EB002026, and the Taplin Fund for Discovery.

References

[1] M.J. Sampson, R.S. Lovell, W.J. Craigen, The murine voltage-dependent anion channel gene family: conserved structure and function, J. Biol. Chem. 272 (1997) 18966–18973.
[2] M.J. Young, D.C. Bay, G. Hausner, D.A. Court, The evolutionary history of mitochondrial porins, BMC Evol. Biol. 7 (2007) 31.
[3] S.J. Schein, M. Colombini, A. Finkelstein, Reconstitution in planar lipid bilayers of a voltage-dependent anion-selective channel obtained from paramecium mitochondria, J. Membr. Biol. 30 (1976) 99–120.
[4] M. Madesh, G. Hajnoczky, VDAC-dependent permeabilization of the outer mitochondrial membrane by superoxide induces rapid and massive cytochrome c release, J. Cell Biol. 155 (2001) 1003–1015.
[5] S. Shimizu, Y. Matsuoka, Y. Shinohara, Y. Yoneda, Y. Tsujimot, Essential role of voltage-dependent anion channel in various forms of apoptosis in mammalian cells, J. Cell Biol. 152 (2001) 237–250.
[6] H. Kusano, S. Shimizu, R. Koya, H. Fujita, S. Kamada, N. Kuzumaki, Y. Tsujimoto, Human gelsolin prevents apoptosis by inhibiting apoptotic mitochondrial changes via closing VDAC, Oncogene 19 (2000) 4807–4814.
[7] J.G. Pastorino, N. Shulga, J.B. Hoek, Mitochondrial binding of hexokinase II inhibits Bax-induced cytochrome c release and apoptosis, J. Biol. Chem. 277 (2002) 7610–7618.
[8] S. Shimizu, M. Narita, Y. Tsujimoto, Bcl-2 family proteins regulate the release of apoptogenic cytochrome c by the mitochondrial channel VDAC, Nature 399 (1999) 483–487.
[9] D.J. Granville, R.A. Gottlieb, The mitochondrial voltage-dependent anion channel (VDAC) as a therapeutic target for initiating cell death, Curr. Med. Chem. 10 (2003) 1527–1533.
[10] V. Shoshan-Barmatz, V.D. Pinto, M. Zweckstetter, Z. Raviv, N. Keinan, N. Arbel, VDAC, a multi-functional mitochondrial protein regulating cell life and death, Mol. Aspects Med. 31 (2010) 227–285.
[11] S. Hiller, J. Abramson, C. Mannella, G. Wagner, K. Zeth, The 3D structures of VDAC represent a native conformation, Trends Biochem. Sci. 35 (2010) 514–521.
[12] S. Hiller, R.G. Garces, T.J. Malia, V.Y. Orekhov, M. Colombini, G. Wagner, Solution structure of the integral human membrane protein VDAC-1 in detergent micelles, Science 321 (2008) 1206–1210.
[13] M. Bayrhuber, T. Meins, M. Habeck, S. Becker, K. Giller, S. Villinger, C. Vonrhein, C. Griesinger, M. Zweckstetter, K. Zeth, Structure of the human voltage-dependent anion channel, Proc. Natl. Acad. Sci. U. S. A. 105 (2008) 15370–15375.
[14] R. Ujwal, D. Cascio, J.P. Colletier, S. Faham, J. Zhang, L. Toro, P. Ping, J. Abramson, The crystal structure of mouse VDAC1 at 2.3 Å resolution reveals mechanistic insights into metabolite gating, Proc. Natl. Acad. Sci. U. S. A. 105 (2008) 17742–17747.
[15] K.-D. Hinsch, V.D. Pinto, V.A. Aires, X. Schneider, A. Messina, E. Hinsch, Voltage-dependent anion-selective channels VDAC2 and VDAC3 are abundant proteins in bovine outer dense fibers, a cytoskeletal component of the sperm flagellum, J. Biol. Chem. 279 (2004) 15281–15288.
[16] E.H.-Y. Cheng, T.V. Sheiko, J.K. Fisher, W.J. Craigen, S.J. Korsmeyer, VDAC2 inhibits BAK activation and mitochondrial apoptosis, Science 301 (2003) 513–517.
[17] N. Yagoda, M. von Rechenberg, E. Zaganjor, A.J. Bauer, W.S. Yang, D.J. Fridman, A.J. Wolpaw, I. Smukste, J.M. Peltier, J.J. Boniface, R. Smith, S.L. Lessnick, S. Sahasrabudhe, B.R. Stockwell, RAS-RAF-MEK-dependent oxidative cell death involving voltage-dependent anion channels, Nature 447 (2007) 864–868.
[18] A.J. Bauer, S. Gieschler, K.M. Lemberg, A.E. McDermott, B.R. Stockwell, Functional model of metabolite gating by human voltage-dependent anion channel 2, Biochemistry 50 (2011) 3408–3410.
[19] C. Fernández, K. Wüthrich, NMR solution structure determination of membrane proteins reconstituted in detergent micelles, FEBS Lett. 27 (2003) 144–150.
[20] P.M. Hwang, W.Y. Choy, E.I. Lo, L. Chen, J.D. Forman-Kay, C.R. Raetz, G.G. Privé, R.E. Bishop, L.E. Kay, Solution structure and dynamics of the outer membrane enzyme PagP by NMR, Proc. Natl. Acad. Sci. U. S. A. 99 (2002) 13560–13565.
[21] A. Arora, F. Abildgaard, J.H. Bushweller, L.K. Tamm, Structure of outer membrane protein A transmembrane domain by NMR spectroscopy, Natl. Struct. Biol. 8 (2001) 334–338.
[22] M. Renault, O. Saurel, J. Czaplicki, P. Demange, V. Gervais, F. Löhr, V. Réat, M. Piotto, A. Milon, Solution state NMR structure and dynamics of KpOmpA, a 210 residue transmembrane domain possessing a high potential for immunological applications, J. Mol. Biol. 385 (2009) 117–130.
[23] B. Liang, L.K. Tamm, Structure of outer membrane protein G by solution NMR spectroscopy, Proc. Natl. Acad. Sci. U. S. A. 104 (2007) 16140–16145.
[24] J.R. Schnell, J.J. Chou, Structure and mechanism of the M2 proton channel of influenza A virus, Nature 451 (2008) 591–595.
[25] Y. Zhou, T. Cierpicki, R.H. Jimenez, S.M. Lukasik, J.F. Ellena, D.S. Cafiso, H. Kadokura, J. Beckwith, J.H. Bushweller, NMR solution structure of the integral membrane enzyme DsbB: functional insights into DsbB-catalyzed disulfide bond formation, Mol. Cell 31 (2008) 896–908.
[26] K. Oxenoid, J.J. Chou, The structure of phospholamban pentamer reveals a channel-like architecture in membranes, Proc. Natl. Acad. Sci. U. S. A. 102 (2005) 10870–10875.
[27] T. Raschle, S. Hiller, T.-Y. Yu, A.J. Rice, T. Walz, G. Wagner, Structural and functional characterization of the integral membrane protein VDAC-1 in lipid bilayer nanodiscs, J. Am. Chem. Soc. 131 (2009) 17777–17779.
[28] I.G. Denisov, Y.V. Grinkova, A.A. Lazarides, S. Sligar, Directed self-assembly of monodisperse phospholipid bilayer nanodiscs with controlled size, J. Am. Chem. Soc. 126 (11) (2004) 3477–3487.
[29] D. Lee, C. Hilty, G. Wider, K. Wüthrich, Effective rotational correlation times of proteins from NMR relaxation interference, J. Magn. Reson. 178 (2006) 72–76.

[30] T.J. Malia, G. Wagner, NMR structural investigation of the mitochondrial outer membrane protein VDAC and its interaction with antiapoptotic Bcl-xL, Biochemistry 46 (2007) 514–525.
[31] X. Xu, W. Decker, M.J. Sampson, M. Colombini, Mouse VDAC isoforms expressed in yeast: channel properties and their roles in mitochondrial outer membrane permeability, J. Membr. Biol. 170 (1999) 89–102.
[32] M. Zizi, M. Forte, E. Blachly-Dyson, M. Colombini, NADH regulates the gating of VDAC, the mitochondrial outer membrane channel, J. Biol. Chem. 269 (1994) 1614–1616.
[33] S. Hiller, G. Wagner, The role of solution NMR in the structure determinations of VDAC-1 and other membrane proteins, Curr. Opin. Struct. Biol. 19 (2009) 396–401.